Journal of Power Sources, 43–44 (1993) 145–155

Recent advances in experimental methods applied to lithium battery researches

C. S. Cha* and H. X. Yang
Department of Chemistry, Wuhan University, Wuhan 430072 (China)

Abstract

Sealed minicells for microelectrode and spectroelectrochemical investigation of liquid cathode depolarizers of lithium batteries were developed. The applicability of these techniques is illustrated with the results of the Li/$SOCl_2$ and Li/SO_2Cl_2 systems studies using these techniques.

Introduction

As the result of the highly corrosive and sometimes explosive characters of the high-energy liquid cathode depolarizers used in lithium batteries, these systems are often considered as unwelcome subjects in the laboratories. In order to make these systems more acceptable to the electrochemistry and spectroscopy laboratories, we have developed a number of sealed minicells and related techniques. Some of these techniques and results of study of mechanism of the Li/$SOCl_2$ and Li/SO_2Cl_2 systems using these techniques are presented in this paper to illustrate their possible application in lithium battery research.

Microelectrode and spectroelectrochemical measurements

The main body of the experimental minicell is a Teflon cylinder with six screw-threaded holes, two in each of the *x*-, *y*- and *z*-directions (Fig. 1(a)). By attaching different fittings to these holes, it can be easily converted to a sealed cell for microelectrode measurement (Fig. 1(b)) or a sealed cell for various spectroelectrochemical measurements, including the long optical path thin-layer electrode (LOPTLE, Fig. 1(c)) and the transparent and reflecting thin-layer cells (Figs. 1(d) and (e)), using either the conventional light beam or the optical fibre-guided beams. The optical fibre technique is especially suitable for the study of high-energy density systems, since optical fibre-coupled experimental cells can be placed in well-protected cages remote from the spectroscopic instruments and experimenters.

Results obtained with the microelectrode in dilute solutions of liquid depolarizers are valuable in elucidating the basic chemistry of these systems, since the interferences caused by the electrode passivation can almost be neglected in dilute solutions. The overall cathode polarization characteristics of the $LiAlCl_4 + SOCl_2$ (dimethylformamide

*Author to whom correspondence should be addressed.

0378-7753/93/$6.00

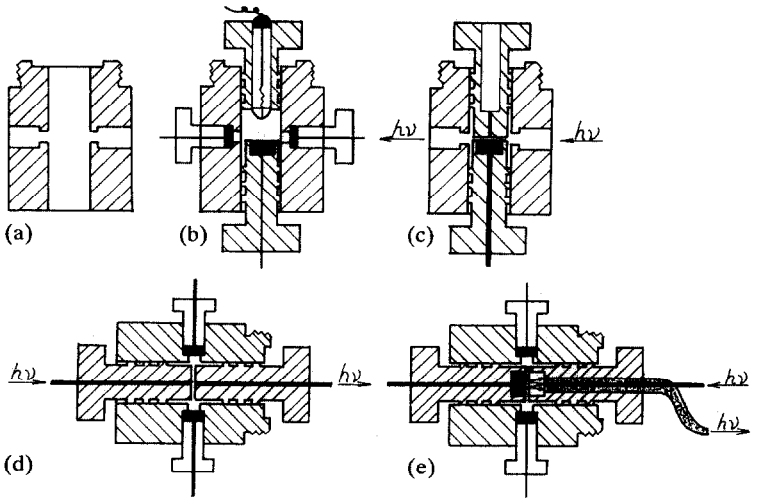

Fig. 1. Experimental sealed minicells: (a) main body, (b) cell for microelectrode, (c) long optical path thin-layer electrode (LOPTLE), (d) transparent thin-layer cell, and (e) reflection thin-layer electrode.

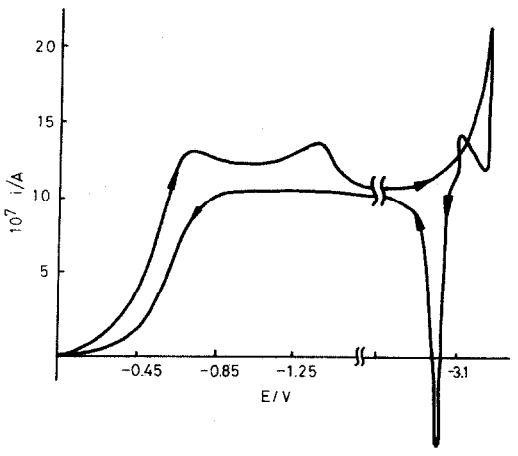

Fig. 2. Wide range cyclo-voltammagram (CV) obtained with $r_0 = 35$ μm platinum microelectrode in 0.11 M $SOCl_2$ + 0.1 M $LiAlCl_4$ in dimethylformamide, scan rate 200 mV/s.

DMF) system in shown in Fig. 2. The main electrochemical events occurring in the potential range 0 to −3.5 V (versus Ag/AgCl) are the following: (i) the 'regular' reduction of $SOCl_2$ in the potential range 0 to −1.0 V; (ii) the further reduction of certain reaction products in the potential range around −1.2 to −1.3 V, and (iii) the deposition and reoxidation of Li in a far cathodic region.

In the region of relatively low polarization, the reduction kinetics of $SOCl_2$ are in good accordance with the theoretical behaviours of the totally-irreversible electrochemical reaction with a Tafel slope of 120–130 mV/decade, suggesting $\alpha = 0.5$ and $n_\alpha = 1$ for the rate-determining step. The total number of electrons (n) involved in

the reduction of $SOCl_2$ can be calculated from the experimental Tafel slope, the limiting diffusion current at the microelectrode I_L and the peak current I_p recorded at high scan rate ($\geqslant$50 V/s). The n value was found to be 2.0$\pm$0.1 [1].

All current–voltage curves measured at $\leqslant$10 mV/s in dilute DMF solutions of $SOCl_2$ show a well-developed diffusion current plateau, so the apparent diffusion coefficient (D_{app}) can be calculated from the steady-state I_L at the microelectrode. Result of such calculation indicated drastic variation of D_{app} in the concentration range $\leqslant$2 mM $SOCl_2$ (Fig. 3). Similar results were reported in ref. 2. However, it is not clear why D_{app} varies in such a way in the extremely low concentration range.

CV in the potential range 0 to -1.0 V displays no anodic peak, indicating that the electrochemical reaction is totally irreversible. Nevertheless, the presence of intermediate of the reaction can be detected spectrophotometrically (Fig. 4(a)), using the LOPTLE technique (Fig. 1(c)). Figure 4(b) shows the gradual raise and fall of

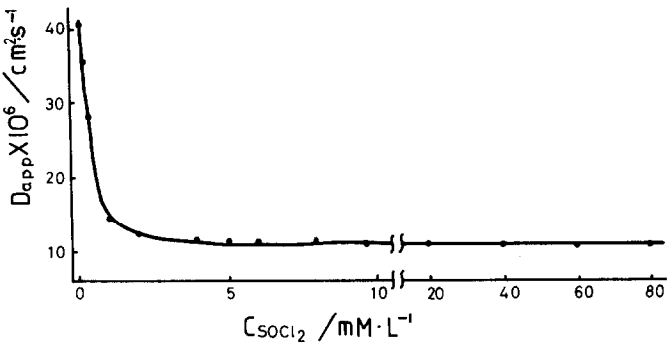

Fig. 3. Calculated D_{app} values.

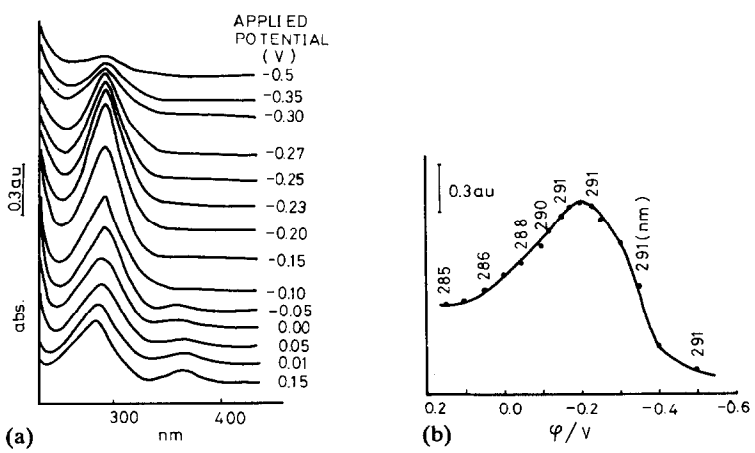

Fig. 4. (a) UV spectra recorded with the long optical path thin-layer electrode (LOPTLE) cell and 2 mM $SOCl_2$+1 M $(C_4H_9)_4NClO_4$ in acetonitrile, and (b) variation of the amplitude and the frequency of the absorption peak; optical path 3 mm, diameter of the platinum electrode 7 mm.

the absorption peak around 290 nm as the electrode potential is scanned from +0.15 to −0.5 V, together with the gradual shift of the peak frequency from 285 to 291 nm. All these results could only be explained by assuming that $SOCl_2$ is consumed in a reduction reaction with the formation of a relatively-stable intermediate, which itself also becomes exhausted as the cathodic polarization is further increased. The fact that the peak at 291 nm varies with potential clearly indicates that the intermediate is decomposed by electrochemical reduction, so it could not be the two-electron reduction product of $SOCl_2$ (such as SO), as suggested in ref. 3.

The second cathodic wave that appears around −1.2 V can only be a further reduction of the product of the first wave, i.e., the two-electron reduction of $SOCl_2$. The peak current increases if the electrode potential is temporarily held at a potential just before the start of the wave [1]. However, the quantity of electricity consumed in the second wave is small, so this wave can be readily observed only at a high rate of potential scanning. The somewhat reversible nature of the second wave is disclosed by the presence of the accompanying anodic peak (Fig. 5(a)). It is interesting to point out that very similar waves can be observed also in dilute solutions of SCl_2 and S_2Cl_2 in DMF (Fig. 5(b)), so very probably the reactive species responsible for the second wave does not contain oxygen.

Spectrophotometric measurements, using the optical fibre-guided reflection thin-layer cell shown in Fig. 1(e), revealed the gradual growth of an absorption peak at 410 nm when the electrode potential was held at −1.4 V (Fig. 6). Simulation of this peak can be achieved with DMF solution containing S_8^{2-} and S_8 (3:1), as shown in the insert in Fig. 6. Therefore, the reaction that gives rise to the second wave is probably the partial reduction of sulfur deposited at the surface of the electrode.

Electrochemical reactions taking place in the potential range around −3.0 V are mainly the deposition and reoxidation of metallic Li. Perhaps the most striking result recorded at the platinum and carbon microelectrodes in DMF containing $LiClO_4$ is that the rate of Li deposition increases very significantly if the solution contains some $SOCl_2$ (Fig. 7). The observed phenomenon cannot be explained as the reoxidation of Li by $SOCl_2$, since the rate of Li deposition is much higher than the limiting diffusion rate of $SOCl_2$. Besides that, the anodic oxidation of deposited Li was found to shift to more positive potential. Thus, a more plausible explaination would be an interaction between deposited Li and the sulfur at the surface of the electrode.

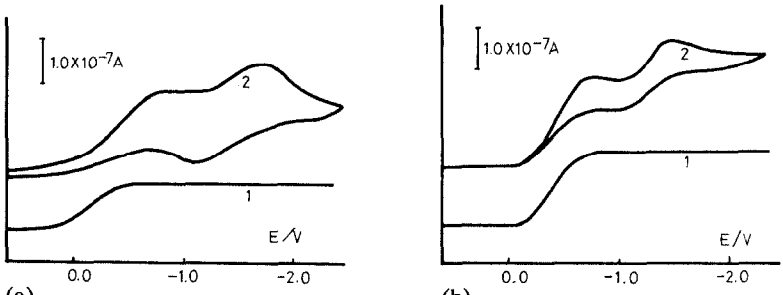

Fig. 5. CV curves measured with $r_0 = 5$ μm platinum microelectrode in dimethylformamide containing: (a) 10 mM $SOCl_2$, and (b) 10 mM SCl_2; scan rate: curve 1, 20 mV/s, and curve 2, 200 mV/s.

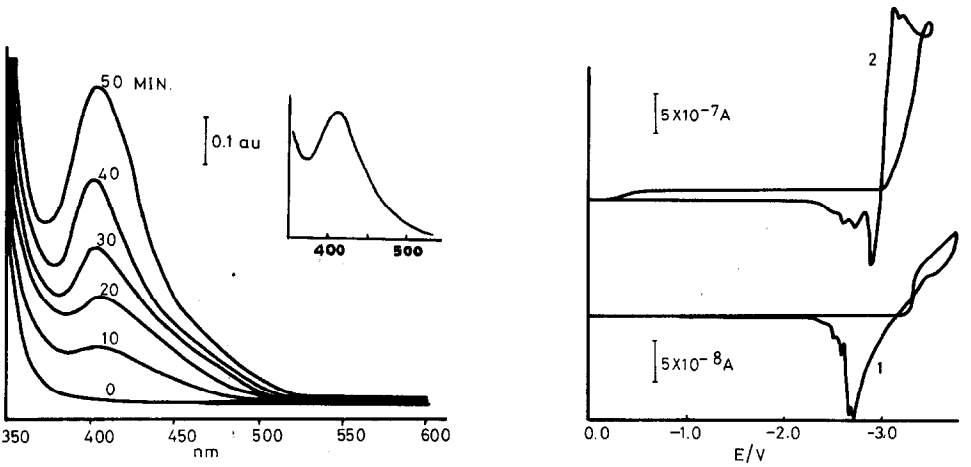

Fig. 6. Variation of the visible spectrum of 0.01 M $SOCl_2$ in dimethylformamide when the electrode potential is held at −1.4 V in a reflection thin-layer cell (Fig. 1(e)). The spectrum of the mixed solution of S_8^{2-} and S_8 (3:1, total concentration 0.01 M) is shown in the box.

Fig. 7. CV curves showing the deposition and reoxidation of lithium; scan rate: 10 mV/s, electrode: $r_0 = 5$ μm platinum microelectrode, solution: 0.5 M $LiAlCl_4$ in dimethylformamide containing (1) no $SOCl_2$, and (2) 20 mM $SOCl_2$.

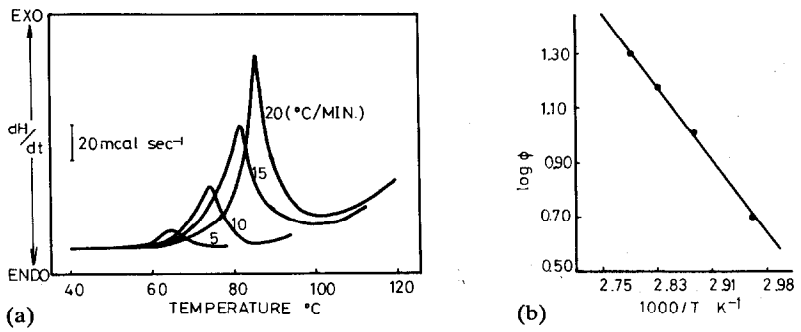

Fig. 8. (a) Differential scanning calorimetry curves of a grey deposite collected from a carbon cathode of a voltage-reversed cathode-limited Li/$SOCl_2$ cell; (b) variation of peak temperature with temperature scan rate.

The above speculation was supported by results of differential scanning calorimetry (DSC) measurement [4]. Moist grey deposits collected from the surface of a carbon cathode of voltage-reversed cathode-limited Li/$SOCl_2$ cell show a distinct exothermic peak at a temperature below 100 °C, and the reciprocal of the peak temperature varies linearly with the logarithm of the temperature scanning rate (Fig. 8(a, b)). Such linear relationship is the general characteristic of detonating materials [5]. Experiments showed that such a low-temperature exothermic reaction can only be simulated with samples in which the Li metal is well-mixed with fine sulfur powder and then moistened with $SOCl_2$ (Fig. 9). The exothermic reaction can be further accelerated by introduction of carbon powder to the mixture (dotted curve in Fig. 9).

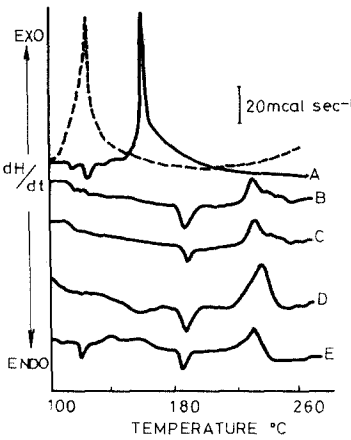

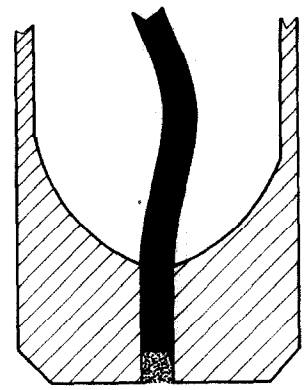

Fig. 9. Differential scanning calorimetry curves of simulated samples: (A) well-mixed Li and S powders, moistened with cell electrolyte; (B) Li sheet mixed with S powder and moistened with cell electrolyte; (C) Li sheet mixed with S powder; (D) well-mixed Li and S powders, and (E) Li moistened with electrolyte.

Fig. 10. Powder microelectrode.

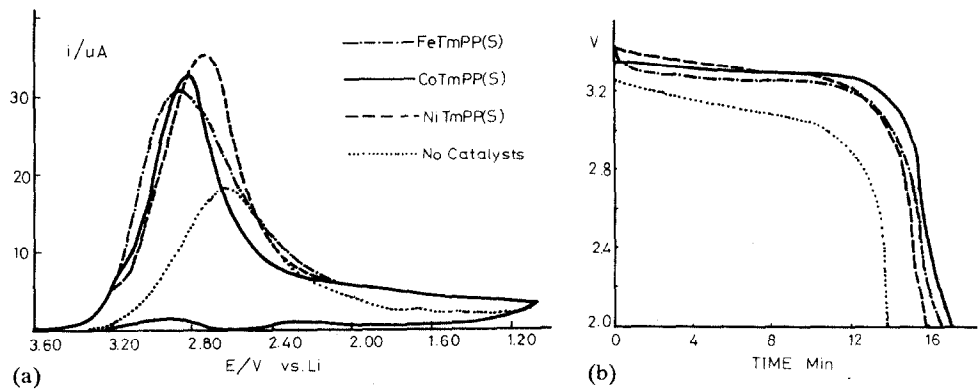

Fig. 11. (a) CV curves obtained at an acetylene black powder microelectrode in 1 M $LiClO_4$ in $SOCl_2$ containing various organometallic additives; (b) discharge curves of $Li/SOCl_2$ cells containing the same additives as in (a).

The current–voltage curves recorded in strong $SOCl_2$ solutions are more complicated and less reproducible as the result of the accompanying process of electrode passivation. Usually, a rather featureless curve with a current peak around -0.5 V is obtained at the carbon fibre microelectrode, and several, more or less overlapping, peaks can be recorded at the platinum microelectrode. These peaks have been assigned in the literature to the reduction of $SOCl_2$, SCl_2, various types of sulfur and various intermediates of the reaction, but spectroscopic evidences were often insufficient. Some additional peaks may appear if the electrode is initially oxidized anodically. These peaks are apparently due to chlorine and chlorinated sulfur compounds such as SCl_2 and S_2Cl_2.

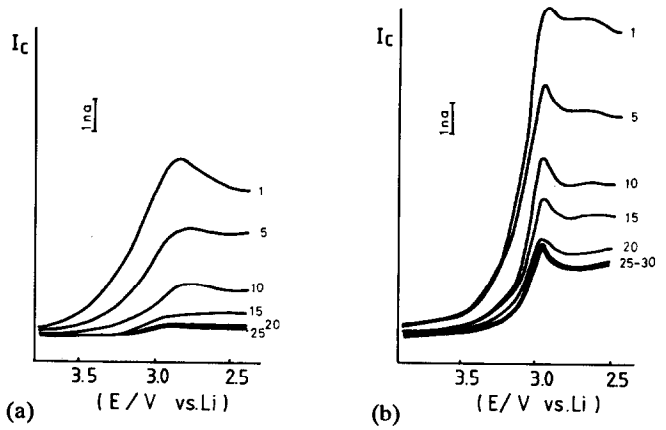

Fig. 12. Successive current–voltage sweeps obtained at $r_0 = 7$ μm carbon fibre in 1.5 M $LiAlCl_4$ in $SOCl_2$ containing: (a) no additive, and (b) 0.1% iron phthalocyanine (FePc).

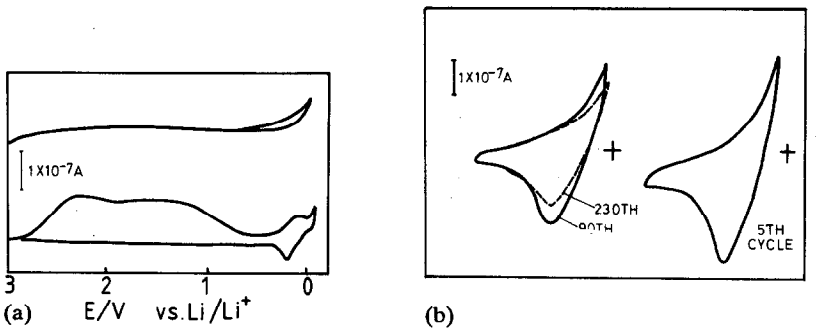

Fig. 13. Current–voltage curves of carbon samples measured with the powder microelectrode technique ($r_0 = 30$ μm), electrolyte: 1 M $LiClO_4$ in 1:1 (v/v) propylene carbonate + dimethoxyethane: (a) active carbon sample, and (b) carbon fabricated by pyrolytic decomposition of benzene at 1000 °C.

In general, current–voltage curves recorded in strong $SOCl_2$ solutions are too complicated to allow the experimenter to draw definite conclusions.

We have also developed in our laboratory a novel type of microelectrode which is especially valuable for the study of powdered samples. The tip of a platinum-wire microelectrode is first etched in aqua regia so that a cavity is formed at the tip. Then powder materials can be packed into that cavity to function as a powder microelectrode (Fig. 10). Some illustrations of the applications of planar and powder microelectrodes in various aspects of Li battery researches are shown in Figs. 11–13.

In Fig. 11 the results of the studies of the effects of macrocyclic organometallic additives with a powder microelectrode and with the conventional discharge curve method are compared.

Figure 12 shows the effect of organometallic additive on the successive current–voltage curves measured with the carbon fibre microelectrode. The decay of reduction current is relatively rapid in solution containing no additive, while in a

solution containing 0.1% iron phthalocyanine (FePc) the rate of decay is slower and a more or less steady state can be reached in which the electrode still maintains a part of its initial activity. This seems to indicate that the organometallic additive works not just as a electrocatalyst.

The powder microelectrode technique is also applicable in the screening of active materials for secondary Li batteries. Figure 13 shows the rechargeability of various carbon samples in a solution containing Li salt. The studied active carbon gives a broad cathodic peak in the first cycle, but the CV curve becomes featureless in the second cycle (Fig. 13(a)). On the other hand, carbon black fabricated by pyrolytic decomposition of benzene at 1000 °C shows much better rechargeability (Fig. 13(b)). More than 50% of the initial capacity could still be retained after 230 cycles.

Raman spectroscopic studies

The *in situ* infrared spectroscopic study of $Li/SOCl_2$ system is often hampered by the rather strong peak due to $SOCl_2$ around 1200 cm^{-1} [6]. Since laser Raman peaks are usually sharper and it is easier to extend the frequency range to 100 cm^{-1} and lower by using the Raman technique, the *in situ* Raman study of the Li/SO_2Cl_2 and the $Li/SOCl_2$ systems has been tried in our laboratory with a sealed transparent minicell made from a 2 mm inner diameter, thin-wall capillary (Fig. 14).

Figure 15 presents the Raman spectra of the liquid phase just above the carbon cathode in a Li/SO_2Cl_2 minicell at various stages of discharge. All the five characteristic peaks of SO_2Cl_2 (220, 284, 414, 570 and 1194 cm^{-1}) are clearly visible at all stages of discharge. The characteristic peaks of $SOCl_2$ (352 and 1240 cm^{-1}) start to appear when the cell has been discharged to 3.0 V. A peak due to SO_2 (1350 cm^{-1}) appears at later stages of discharge and diminishes after cell voltage reversal, indicating a

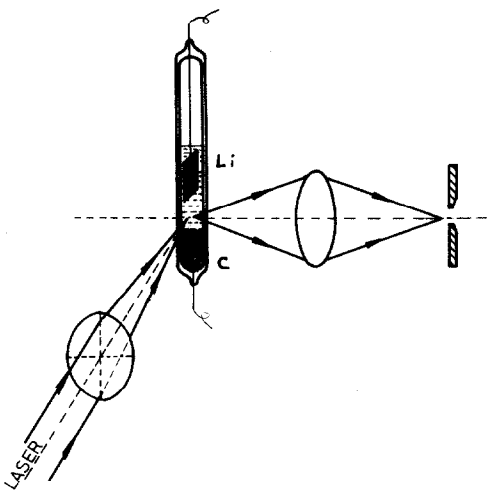

Fig. 14. Sealed minicell for Raman studies.

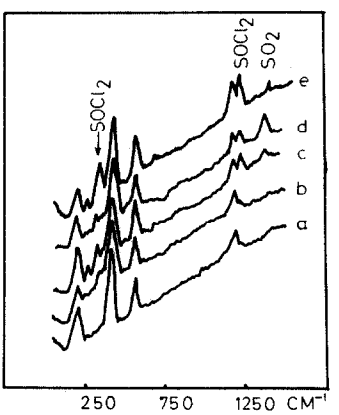

Fig. 15. Raman spectra of an electrolyte in mini-Li/SO_2Cl_2-cell at different stages of discharge: (a) before discharge; (b) discharged to 3.7 V; (c) discharged to 3.0 V; (d) discharged to 0.7 V, and (e) after voltage reversal (−0.7 V); electrolyte: 1.2 M $AlCl_3$ in SO_2Cl_2.

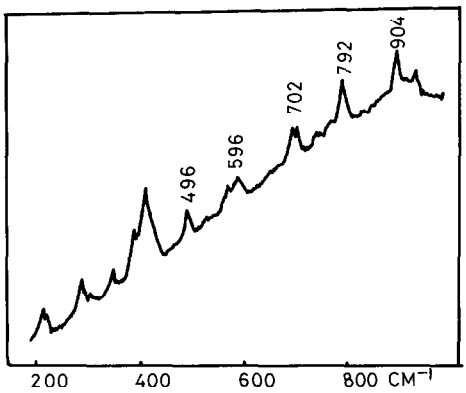

Fig. 16. Raman spectrum of the electrolyte in the Li/SO_2Cl_2 minicell after recharge.

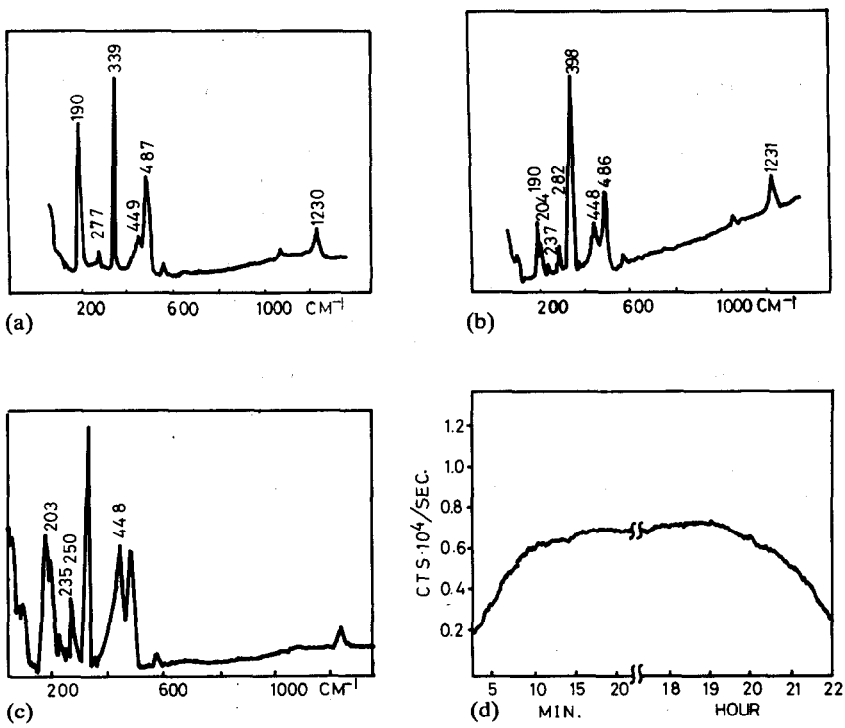

Fig. 17. Raman spectra of the electrolyte in the $Li/SOCl_2$ minicell after discharged to (a) 3.4 V, (b) 3.1 V, and (c) 2.85 V. The variation of the amplitude of the the 448 cm^{-1} peak during the discharge process is shown in (d).

further reduction of SO_2. No new peak has been observed after a prolonged discharge at -0.7 V (i.e., after cell voltage reversal).

A set of new peaks appears in the Raman spectrum of Li/SO_2Cl_2 minicell after recharge (Fig. 16). Among them the peak at 496 cm^{-1} is situated in the characteristic

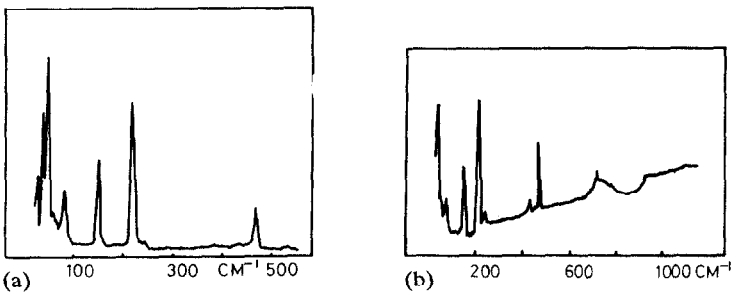

Fig. 18. Raman spectra of the pale yellow crystallites found in pores of discharged carbon cathode of $Li/SOCl_2$; electrolyte: 1.8 M $LiAlCl_4$ in $SOCl_2$ containing (a) no additive, and (b) organometallic additive.

frequency range of S–Cl bond (probably due to SCl_2 or S_2Cl_2), and the peak at 596 cm^{-1} is most probably due to Cl_2. The three new peaks in the 700–900 cm^{-1} range should be noteworthy from the safety point of view, since many compounds containing Cl–O bond show Raman peaks in this frequency range.

The Raman spectra of the electrolyte of the $Li/SOCl_2$ minicell at various stages of discharge are shown in Figs. 17(a)–(c). The most noticeable change of the spectrum accompanying the discharge process is the change of the amplitude of the 448 cm^{-1} peak, which is most probably due to S_2Cl_2. The time variation of the amplitude of this peak is shown in Fig. 17(d), supporting the assumption that S_2Cl_2 is an intermediate of the cell reaction [7].

Characterization of crystallites formed within the porous carbon electrode can be achieved by using the microscopic Raman probe. The Raman spectrum of the pale yellow crystallite found in the pores of the discharged cathode is in perfect accordance with that of orthorhombic S_8 [8], as shown in Fig. 18(a). Abraham [9] had come to the same conclusion by using the X-ray diffractometry method. We have also found that, after the introduction of the organometallic additive to the electrolyte of the $Li/SOCl_2$ cell, the shape of the yellow crystallites became blurred and the Raman spectrum changed significantly (Fig. 18(b)). The new broad peak around 700–800 cm^{-1} is probably an indication of the presence of polydisulfur $(S_2)_n$ chain [10].

Acknowledgements

The work reported in this paper has been supported by the Chinese Nature Sciences Foundation and the Chinese State Educational Committee. Most experimental results were taken from the Ph.D. theses of C. M. Li (1987), F. P. Zhong (1991) and X. J. Xiao (1992), worked out at the Chemistry Department of the Wuhan University.

References

1 C. M. Li and C. S. Cha, *J. Electroanal. Chem., 260* (1989) 91.
2 Y. M. Choi and S. M. Park, *Ext. Abstr., Meet. Electrochemical Society, Phoenix, AZ, USA, Oct. 1991,* Vol. 91–92, Abstr. No. 98.

3 W. L. Bowden and A. N. Dey, *J. Electrochem. Soc., 127* (1980) 1419.
4 Y. J. Xiao, H. X. Yang and C. S. Cha, submitted to *Appl. Chem. (China).*
5 M. I. Pope and M. D. Judd (eds.), *Differential Thermal Analysis,* Heyden and Son, London, 1977, Ch. 23.
6 A. I. Attia, C. Sarrazin, K. A. Gabriel and R. P. Burns, *J. Electrochem. Soc., 131* (1984) 2543.
7 C. A. Hayes, S. L. Gust, M. D. Farrinton and J. A. Lockwood, in A. N. Dey (ed.), *Lithium Batteries,* The Electrochemical Society, Proc. Vol. 87–1, 1987, p. 107.
8 G. A. Ozim, *J. Chem. Soc. A, 100* (1969) 116.
9 K. M. Abraham, M. Alamgir and E. B. Willsteadt, *J. Electrochem. Soc., 137* (1990) 1491.
10 R. E. Bariatta and C. W. Brown, *J. Phys. Chem., 75* (1971) 4059.